An Energy Analysis in Transient Pool Boiling Experiments at Short Durations

Ahmadreza Ayoobi*, Abbas Afshari, Mohammad Farmani

Department of Aerospace Engineering, Shahid Sattari Aeronautical University of Science and Technology, Tehran, Iran

ABSTRACT: In this investigation, the performance of coolant in various operating conditions was examined through an energy analysis of experimental data. A novel method was introduced for presenting pool boiling test results, facilitating coolant performance assessment across distinct operational scenarios and enabling comparative energy analyses between transient and steady-state boiling. Leveraging principles of thermal science, distinct correlations were formulated to elucidate pool boiling phenomena in transient mode. analysis was based on experimental results from transient pool boiling tests conducted over predefined time intervals. analysis indicates a direct correlation between the heater's energy output and test duration. Notably, in a steady state, the energy rate produced as a result of Joule heating effects reached its maximum value, which is reflective of the extended duration of this state relative to transient state tests. Specifically, energy yield from the wire heater increased by 75% when the test duration was extended from 1s to 5s. Furthermore, extending duration to 10 s increased energy outputs by 62% and 186% compared to 5s and 1s durations, respectively. Performance decreases as a vapor film forms temporarily, before increasing and becoming nearly constant during film boiling.

1- Introduction

The boiling phenomenon is one of the effective ways of heat transfer in heat generation systems such as power plants, automobiles, electronic equipment, etc. The boiling phenomenon is accompanied by phase change from liquid to vapor at saturation temperature. Much scientific research has been related to the boiling phenomenon due to its cheapness and widespread use in industry and daily life, so many papers have been published yearly. The only limitation of this heat transfer is that critical heat flux occurs, limiting its use in industry. Critical heat flux occurs at the end of the nucleate boiling regime, followed by transition and film boiling regimes where the heat transfer coefficient decreases. Also, the nucleate boiling regime's onset is one of the parameters that must be considered in boiling analysis due to adverse effects (thermal shocks) on the long-term stable operation of the system's life.

Most research on pool boiling mainly concentrates on steady-state mode and pays less attention to transient mode. Studying pool boiling in experimental setups involves distinguishing between steady-state and transient modes. In steady-state mode, time taken for research is not a factor, and heat flux rises gradually depending on the stability of heater temperature, usually spanning from 3 to 7 minutes. On the other hand, during the transient mode, research duration is fixed, and heat flux increases as per the designated time for each test. Ayoobi et al. [1-5] experimentally studied pool boiling heat transfer and critical heat flux (CHF) in subcooled temperatures ranging from 0 to 20 under transient power conditions. They linearly changed heating rates in the test section depending on the scheduled duration of the voltage control from 1 to 1000. Their results showed that the transient boiling heat transfer coefficient increases in the nucleate boiling region in all durations. They claimed it is due to bubbles' growth, separation, motion, and turbulence. They used a high-speed camera to capture bubble and vapor film behavior around the heating wire. In another research, they studied pool boiling heat transfer and critical heat flux (CHF) in ferrofluid under transient power conditions. They discussed the results of transient boiling heat transfer coefficient, transient CHF, scanning electronic microscopy (SEM) images of surface wire, and high-speed camera images. By up to 100 seconds, CHF and wire superheat temperatures at CHF point decrease with increasing duration, and incipient boiling point falls. In addition, they showed that the heat transfer coefficient decreases due to high heat flux and vapor film thickness around the wire in the second part of the film boiling. Moreover, they experimentally studied pool boiling heat transfer and critical heat flux in saturated water under transient power conditions. Their results showed that, at first, the transient boiling heat transfer coefficient increases in the nucleate boiling region. Then, it decreases in

*Corresponding author's email: ar.ayoobi@ssau.ac.ir

transition from the nucleate boiling region to the film boiling region. Finally, it rises in the film boiling region. Also, the incipient boiling point decreases, which they explained by a reduction in nucleation sites and the explosive nature of the initial nucleate boiling stage in transient boiling. The quest to enhance heat transfer efficiency in various engineering applications has spurred a series of innovative studies focused on the effects of surface wettability and structural modifications. One notable investigation by Deb et al. [6] meticulously examined the impact of surface wettability on nucleate boiling heat transfer across Silicon Dioxide thin film nanocoated surfaces. Their research revealed a significant reduction in wall superheats, coupled with an enhancement in heat transfer coefficients for all examined nanocoated surfaces compared to traditional plain surfaces, all while utilizing saturated refrigerant R-141b as a working fluid. Exploring further into the realm of boiling heat transfer, Naphon and Thongjing [7] expanded upon this foundation, investigating characteristics of pool boiling using both refrigerant R-141b and ethyl alcohol. Their findings underscored how nanoparticle concentration and boiling pressure intricately influenced pool boiling heat transfer coefficient, thereby illuminating the complex relationship between fluid properties and surface characteristics. Continuing this trajectory, Bock et al. [8] conducted a comprehensive study assessing the thermal performance of three nanostructured and two uncoated surfaces while employing refrigerants R-134a and R-245fa. Their investigation indicated that a commercially applied nanocoating process yielded the highest heat transfer coefficients, whereas both nanocoated tubes and polished surfaces demonstrated the lowest efficiency, shedding light on the crucial role of surface treatment in thermal management. In a bid to understand the mechanics behind nucleate pool boiling, Kim and Kim [9] developed a mechanistic model that addressed the effects of bubble coalescence on heat transfer. Their exploration revealed how bubble dynamics could modify area fractions related to quenching and evaporation, significantly impacting heat transfer efficiency based on wall superheat conditions. Gouda et al. [10] took a different perspective by investigating the effect of surfactants deposited on heating surfaces during pool boiling with deionized water. Their results highlighted an intriguing transition: surfaces treated with surfactants exhibited roughness levels 4 to 10 times greater than that of fresh heating surfaces, showing an increase in wettability that contributed positively to boiling performance. A further exploration of time dependencies in pool boiling was undertaken by Li et al. [13], examining variations in heat transfer coefficients and fouling resistance over a substantial duration of 1000 minutes. Their experimental work illuminated initial improvements in thermal conductivity, followed by a decline attributed to the formation of a fouling layer, marking an essential consideration in practical applications. Investigations into bubble dynamics led Righetti et al. [14] to reveal that, despite resistance to bubble escape, pool boiling on 10 mm foam aluminum demonstrated augmented heat transfer capabilities in deionized water compared to flat plates. Utilizing high-speed cameras, they adeptly visualized the interplay between bubble dynamics and foam geometry. Adding to a growing body of knowledge, Betz et al. [15] focused on the performance of biophilic surfaces, elucidating how regions of differing wettability provided superior heat transfer coefficients and critical heat fluxes exceeding 100 W/cm². Similarly, Li et al. [16] innovatively employed photolithography and electrochemical deposition to engineer ultrasmall microchannels in copper, discovering a linear correlation between contact line increase and critical heat flux, showcasing a remarkable 930% enhancement in heat transfer coefficient at a mere 5 °C wall superheat. Finally, a study by Mata et al. [17] on the influence of surface roughness in copper tubes during pool boiling revealed a noteworthy finding: rough surfaces facilitated a 1.5 times greater heat transfer coefficient and larger bubble departures. Complementing these insights, Zakšek et al. [18] investigated nucleate boiling on both smooth and laser-textured stainless-steel foils. Their results indicated that while smooth surfaces exhibited lower heat transfer coefficients and higher activation temperatures, laser-textured foils demonstrated enhanced boiling performance, underscoring the potential of surface engineering in optimizing thermal efficiency. Through these various studies, the intricate relationship between surface modifications, wettability, and heat transfer performance has become increasingly clear, paving the way for innovations that could significantly elevate thermal management systems across multiple domains.

Investigation of previous research reveals an under-researched and under-explored aspect within pool boiling analysis, which has historically focused on general parameters such as heat flux, critical heat flux, heat transfer coefficient, and superheat temperature. Existing studies have provided limited and usual insights based on these parameters. This paper embarks on a thorough exploration of boiling phenomena by harnessing data obtained from experimental studies. An analysis is approached from an energy perspective, aiming to establish connections among energy generated, transferred, and stored during boiling. Novel formulations have been developed to introduce a groundbreaking parameter for assessing a working fluid's ability to absorb heat from a heater, particularly in the context of pool boiling. This parameter serves as a measure of the fluid's capacity and capability in this regard. Experimental results based on these derived formulas and new criteria are presented in innovative figures, with their behavior elucidated. Coolant performance, evaporated mass rate, and stored, generated, and transferred energy during different time frames in transient mode have been meticulously computed and thoroughly discussed.

2- Laboratory equipment

Results of ref. [5] are used as transient pool boiling experiments in scheduled durations. Equipment including three power supplies, a high-speed data acquisition card, a personal computer, a hot plate, a boiling vessel, copper electrodes, wire as a heater, a condenser, power, control, and amplified circuits were used to investigate transient boiling.

A power supply (GPC-3060D, Gwinstek Co., Ltd) was used to provide the required power to the power circuit, and two power supplies (Hy3020, Huayi Electric Co., Ltd) were used to provide power to the amplifier circuit. The task of the power circuit is to provide the required energy, which is scheduled in the control circuit according to the designed duration to supply the wire heater. The control circuit created a voltage potential difference on the wire heater, resulting in an electrical current flow in the wire heater. Different transient conditions were scheduled for transient boiling using a control circuit. A program coded in a control circuit provides the requirements the designer desires for several experiments. The experiment's start power, end power, start time, and end time were specified using its keyboard. A boiling vessel keeps electrodes and wire heater in position and deionized water at a desired temperature. It is made of Pyrex and placed on a hot plate. Pyrex material can withstand high temperatures and is transparent to observe and photograph its inside. Using an amplifier circuit, the value of the voltage potential difference on shunt 40 mΩ is magnified to be in the measurement range of a high-speed data acquisition card. The temperature of deionized water inside the boiling vessel reaches saturation temperature by the hot plate. The hot plate has a PT 1000 thermocouple to continuously measure fluid temperature and keep fluid at saturation temperature. A high-speed data acquisition card (Advantech pci-1716) with a maximum speed of 250 kHz and 16-bit accuracy is used to measure and save voltage potential difference between wire heater and shunt on a personal computer. To keep a constant level of deionized water, a condenser is used, though the amount of evaporated water returns to a working fluid, and as a result, conditions inside the boiling vessel are the same during experiments. Two electrodes are applied to hold the wire heater horizontally and connect the control circuit to the wire heater.

Wire heater has a diameter of 0.15 mm and a length of 650 mm. During experiments, the wire heater reaches a melting point and is cut down, and as a result, a new wire is used for each experiment. In steady mode, the voltage potential difference is increased in steps of 1 V every 5 min. And consequently, electrical current is increased. Wire resistance and, as a result, wire temperature changes due to increased voltage potential difference and electrical current. In this method, the criterion of waiting time to the next step of voltage potential difference is that surface temperature be constant, which in this equipment is 5 min. is enough. Also, the voltage potential difference increment in steady boiling is continued until the wire heater. In transient boiling, the voltage potential difference on the wire heater is changed linearly using the control circuit from 0 to 50 V during scheduled duration t (s). Durations are including 1, 5, and 10s. During the boiling experiment, the value of voltage potential difference and electrical current with suitable frequency were recorded, which was used to calculate wire resistance and temperature in each instant. More details were explained in ref. [5]. The relation between wire resistance and temperature is as follows:

$$\overline{T}_{wire}(t) = \frac{\overline{R}_{wire}(t) - R_{0_{wire}}}{\alpha R_{0_{wire}}} + T_0 \tag{1}$$

Where $T_0, R_0, \alpha, \overline{T}_W(t)$ are reference temperature, reference resistance, temperature-resistance coefficient (obtained experimentally), and instantaneous wire temperature, respectively. In the above relation $\overline{R}_{wire}(t)$ is instantaneous wire resistance calculated from the Ohm relation:

$$\overline{R}_{wire}(t) = \frac{\overline{\Delta V}}{\overline{I}} \tag{2}$$

The energy balance for the wire heater gives:

$$\dot{E}_{gen_{wire}} - \dot{E}_{out_{wire}} = \dot{E}_{store_{wire}} \tag{3}$$

In the above equation, generated energy and stored energy inside the wire heater are calculated from eq. (4) and (5):

$$\dot{E}_{gen_{wire}} = VI \tag{4}$$

$$\dot{E}_{store_{wire}} = \rho_{wire} \forall_{wire} C_{wire} \frac{dT_{wire}}{dt} \tag{5}$$

Where and are electrical voltage and current in eq. (4). In addition, $\rho_{wire}, \forall_{wire}$, and C_{wire} are wire density, wire volume, and specific heat capacity of wire in eq. (5). Therefore, output energy ($\dot{E}_{out_{wire}}$) calculated from eq. (6):

$$\dot{E}_{out_{wire}} = VI - \rho_{wire} \forall_{wire} C_{wire} \frac{dT_{wire}}{dt} \tag{6}$$

In addition, the energy balance for deionized water as a coolant, which assumes a closed system, gives:

$$\dot{E}_{in} - \dot{E}_{out} = \frac{dE}{dt} \tag{7}$$

Energy change of deionized water is zero at saturation temperature

$$\left(\frac{dE}{dt} = \frac{d}{dt}(mCT) = CT\frac{dm}{dt} + mT\frac{dC}{dt} + mc\frac{dT}{dt} = 0\right).$$

Phase change and water evaporation occur by each value of entered energy to deionized water, resulting in water temperature not changing.

$$\dot{E}_{in_{water}} - \dot{E}_{out_{evap}} = 0 \tag{8}$$

$$\dot{E}_{in_{water}} = \dot{E}_{out_{evap}} \tag{9}$$

The total evaporated mass rate and total evaporated mass at a specific time may be found from eq. (10) and (11) respectively:

$$\dot{M}_{evap}(t) = \frac{\dot{E}_{in_{water}}}{H_{fg}} \tag{10}$$

$$M_{evap} = \int_{t=0}^{t} \dot{M}_{evap}(t)dt \tag{11}$$

Defining a relation for cooling by referencing eq. (12) and (13) as coolant performance:

$$\eta_I = \frac{given\ energy}{total\ generated\ energy} \tag{12}$$

$$\eta_I = \frac{\dot{E}_{in_{water}}}{\dot{E}_{gen_{wire}}} = 1 - \frac{\rho_{wire}\,\forall_{wire}\,C_{wire}\dfrac{dT_{wire}}{dt}}{\dot{E}_{gen_{wire}}} \tag{13}$$

Also, total stored and generated energies may be found in eq. (14) and (15):

$$E_{store_{wire}} = \int_{t=0}^{t} \rho_{wire}\,\forall_{wire}\,C_{wire}\frac{dT_{wire}}{dt}dt \tag{14}$$

$$E_{gen_{wire}} = \int_{t=0}^{t} \dot{E}_{gen_{wire}}dt \tag{15}$$

Therefore, total coolant performance for each condition may be found by:

$$\eta_I = \frac{E_{in_{water}}}{E_{gen_{wire}}} = 1 - \frac{E_{store_{wire}}}{E_{gen_{wire}}} \tag{16}$$

Heat flux value is calculated using wire superheat temperature ($\Delta T_{wire} = \overline{T}_{wire} - T_{sat}$):

$$q'' = \frac{v}{A_w}\left(\frac{\overline{I\Delta V}}{v} - \rho_{wire}\,\forall_{wire}\,C_{wire}\frac{dT_{wire}}{dt}\right) \tag{17}$$

In this research, to evaluate uncertainty, the Moffat [19] method is applied (from eq. (19) to eq.(22)). Also, knowing voltage potential difference and shunt resistance, electrical current is calculated by eq. (18)

$$\overline{I} = \frac{\overline{\Delta V}}{R_{shunt}} \tag{18}$$

$$\frac{U_{v_{wire}}}{V_{wire}} = \left[\left(\frac{U_r}{r}\right)^2 + \left(\frac{U_l}{l}\right)^2\right]^{0.5} \tag{19}$$

$$\frac{U_{T_{wire}}}{T_{wire}} = \left[\left(\frac{U_{\Delta V}}{\Delta V}\right)^2 + \left(\frac{U_{\overline{I}}}{R_{shunt}}\right)^2\right]^{0.5} \tag{20}$$

$$\frac{U_I}{I} = \left[\left(\frac{U_{\Delta V}}{\Delta V}\right)^2 + \left(\frac{U_{R_{shunt}}}{R_{shunt}}\right)^2\right]^{0.5} \tag{21}$$

$$\frac{U_{E_{gen_{wire}}}}{E_{gen_{wire}}} = \left[\left(\frac{U_{\Delta V}}{\Delta V}\right)^2 + \left(\frac{U_I}{I}\right)^2\right]^{0.5} \tag{22}$$

Uncertainty values for wire volume, wire temperature, voltage potential difference, electrical current, and generated energy are calculated to be approximately 2.3%, 0.17%, 0.35%, 0.57%, and 0.77%, respectively.

Rohsenow [20] and Zuber [21] correlations validate nucleate boiling regime and CHF in empirical works, respectively shown in eq. (23) and (24):

$$\Delta T_s = \frac{h_{fg}}{C_{p,l}}C_{sf}\left[\frac{q''}{\mu_l h_{fg}}\left(\frac{\sigma}{g(\rho_l - \rho_v)}\right)^{0.5}\right]^{\frac{1}{3}} pr^n \tag{23}$$

$$q''_{CHF} = 0.131 h_{fg}\rho_v^{0.5}(g\sigma(\rho_l - \rho_v))^{0.25} \tag{24}$$
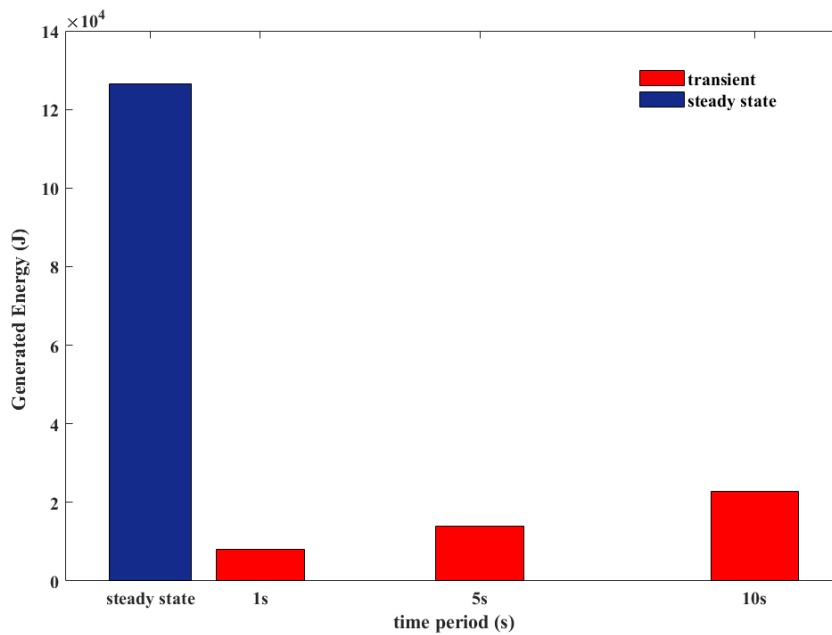
Fig. 1. Generated energy in wire heater at durations of 1, 5, and 10s and steady mode

3- Results

It was shown (ref. [5]) that steady mode of pool boiling experiment results that compare with eq. (23) and eq. (24) for nucleate boiling regime and CHF value, respectively. It was validated that experimental heat flux follows Rohsenow's [20] correlation, and experimental CHF occurs close to predicted CHF by Zuber's [21] correlation.

Fig. 1 shows the energy amount generated in each duration in transient and steady modes. As can be seen, the amount of generated energy increased with increasing duration. Generated energy in steady mode is the maximum value because the experimental time of steady mode is higher than other durations in transient mode. Experiment times for scheduled 1s, 5s, and 10s are 520 ms, 2120 ms, and 4040 ms, respectively, indicating that experiments concluded earlier than scheduled durations. The experiment time of steady mode lasts 4500 s. Generated energy in wire heater at a duration of 5s increases by 75% compared to the duration of 1s, and at the duration of 10s, generated energy increases by 62% and 186% compared to the duration of 5s and 1s, respectively. The duration of 5s is five times bigger than a duration of 1s, and the duration of 10s was two times the duration of 5s; the generated power increase in the wire was not proportional to the duration increase.

Behaviours between wire heater surface and working fluid at different durations are complicated and depend on the duration of heat transfer regimes like the nucleate boiling regime and working fluid time behaviour compared to received energy. Therefore, these results show that heat transfer mechanisms in pool boiling with working fluid of water concerning the duration of input energy changes in different durations. Those changes may be related to different numbers of nucleate sites and generated bubble rates in related regimes.

Figs. 2 and 3 indicate the generated energy rate for 1, 5, and 10s versus normalized and non-normalized experiment duration. As can be seen, the amount of generated energy rate decreases with increasing duration. This is due to the amount of generated energy reducing with time due to increased experiment duration. According to Fig. 3 and 4, it can be seen that although the generated energy rate at the duration of 1s is highest, the amount of generated energy is lowest. Also, a second-order polynomial function can be fit on the generated energy rate in all durations since voltage potential difference and electrical current are increased linearly.

stored energy in the wire heater is shown in Fig. 6 for transient and steady modes. From Fig. 4, the stored energy value decreases with increasing duration in the transient mode of boiling. At a duration of 5s, stored energy reduces by 10% in comparison to a duration of 1s. At a duration of 10s, stored energy reduces by 42% in comparison to a duration of 5s. In comparison to Fig. 3, it can be seen that while generated energy at the duration of 1s is the lowest, stored energy is the highest among other durations. Therefore, the generated energy value is low in fast heating, most of which is stored in wire. This relation decreases in other durations. Also, it is found that the heat transfer value at the duration of 1 is less than the duration of 5 and 10s. In addition, stored
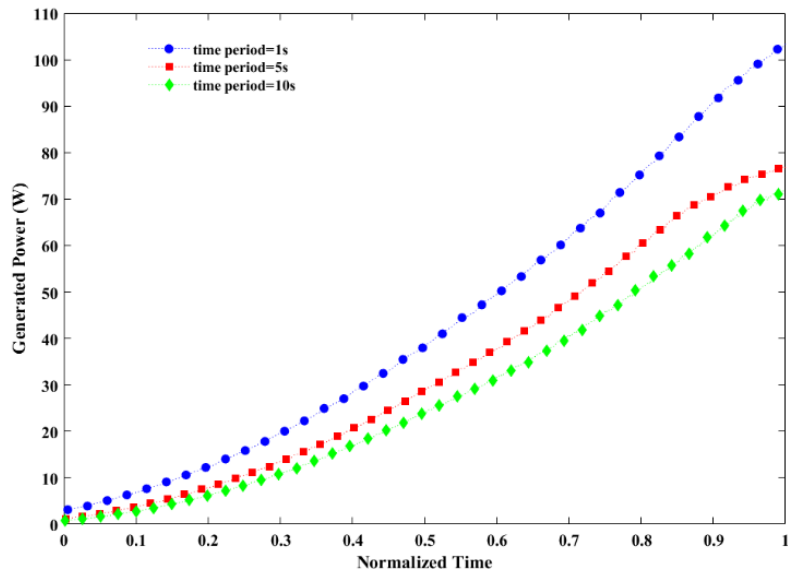
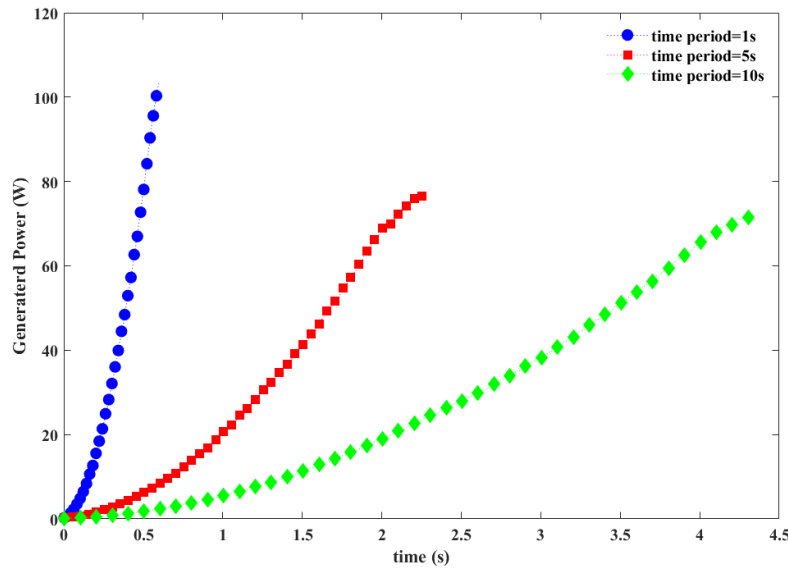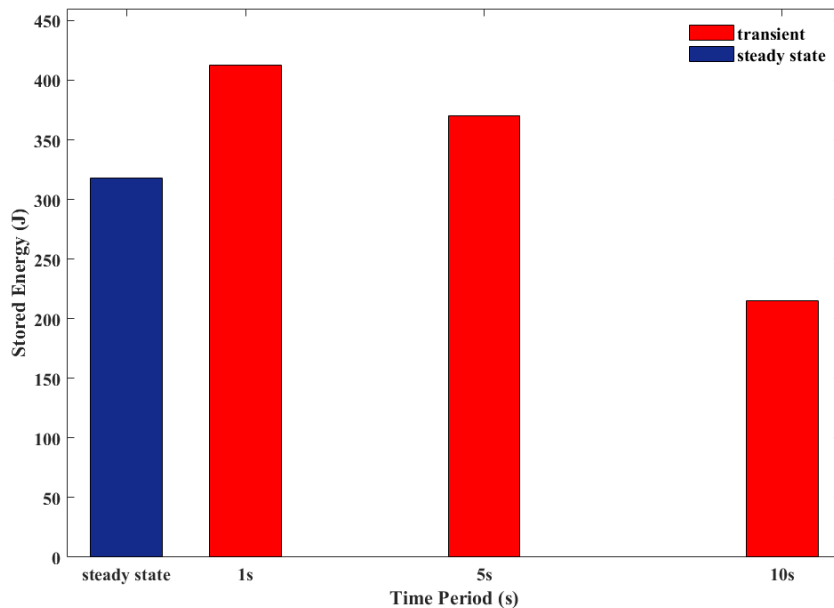**Fig. 2. generated energy rate versus normalized time for 1, 5, and 10 s.**

Fig. 3. generated energy rate versus non-normalized time for durations of 1, 5, and 10s

Fig. 4. stored energy in the wire at durations of 1s, 5s, 10s, and steady mode

energy in steady mode is less than durations of 1s and 5s of transient mode, indicating heat transfer increases in steady mode relative to transient mode (short durations). Therefore, duration can be scheduled and optimized to less stored energy, resulting in more output energy from the wire heater in transient boiling mode.

experiment results in the following figures are not smooth because each data belonged to the entire wire surface, and wire surface temperature at each duration is different according to ref. [22]. During steady mode of boiling, Sedmak et al. [22] indicated that temperature distribution under bubbles on the surface during bubble growth is changed up to 5 K. Temperature distribution of surrounding liquid is changed up to 7 K. This research shows that superheat temperature variation of giant bubble that contacts surface reached 1 K during 9.7 ms. Non-smooth curve at the duration of 1s is higher than other durations due to the duration of bubble growth being very fast, which results in the temperature distribution of the wire surface and surrounding liquid changing considerably. In addition, temperature derivative concerning duration noticeably changes stored energy, output energy, and coolant performance data.

Fig. 5 shows the stored energy rate in the wire heater at 1, 5, and 10s versus normalized experiment duration. As can be seen, first, the stored energy rate is high and decreases gradually. This trend belongs to the free convection regime, with low heat transfer from wire to deionized water. Then, in

the nucleate boiling regime, the stored energy rate decreases significantly as almost all of the generated energy transfers to deionized water, and also, its trend is not highly changed. Next, the stored energy rate increases considerably related to the CHF point. Then, the heat transfer coefficient decreases in the transition regime, where vapor layers form temporarily on the wire surface. After that, the stored energy rate again reduces steadily, and finally, in the film boiling regime, due to the formation of a vapor film around the wire, the stored energy rate increases until the wire temperature reaches a melting point and the wire is torn suddenly. Compared to the amount of stored energy, the peak of stored energy (at CHF) decreases by increasing duration, shown in Fig. 12 of ref. [5]. The maximum amount of stored energy rate in the wire is in film boiling, then CHF point, and finally, in free convection boiling regime. The stored energy rate in the nucleate boiling regime and the first part of film boiling are approximately steady (no remarkable ups and downs). Due to extreme phase change at the nucleate site and the whole activity of sites, stored energy is approximately unchanged. Also, in the first part of the film boiling due to the thin film about wire, the stored energy rate is low and constant, and then, due to the formation of a thick film about wire, stored energy increases (insufficient heat transfer coefficient).

The amount of output energy from the wire for transient and steady modes is shown in Fig. 6 As can be seen, the amount of output energy increases with increasing duration.
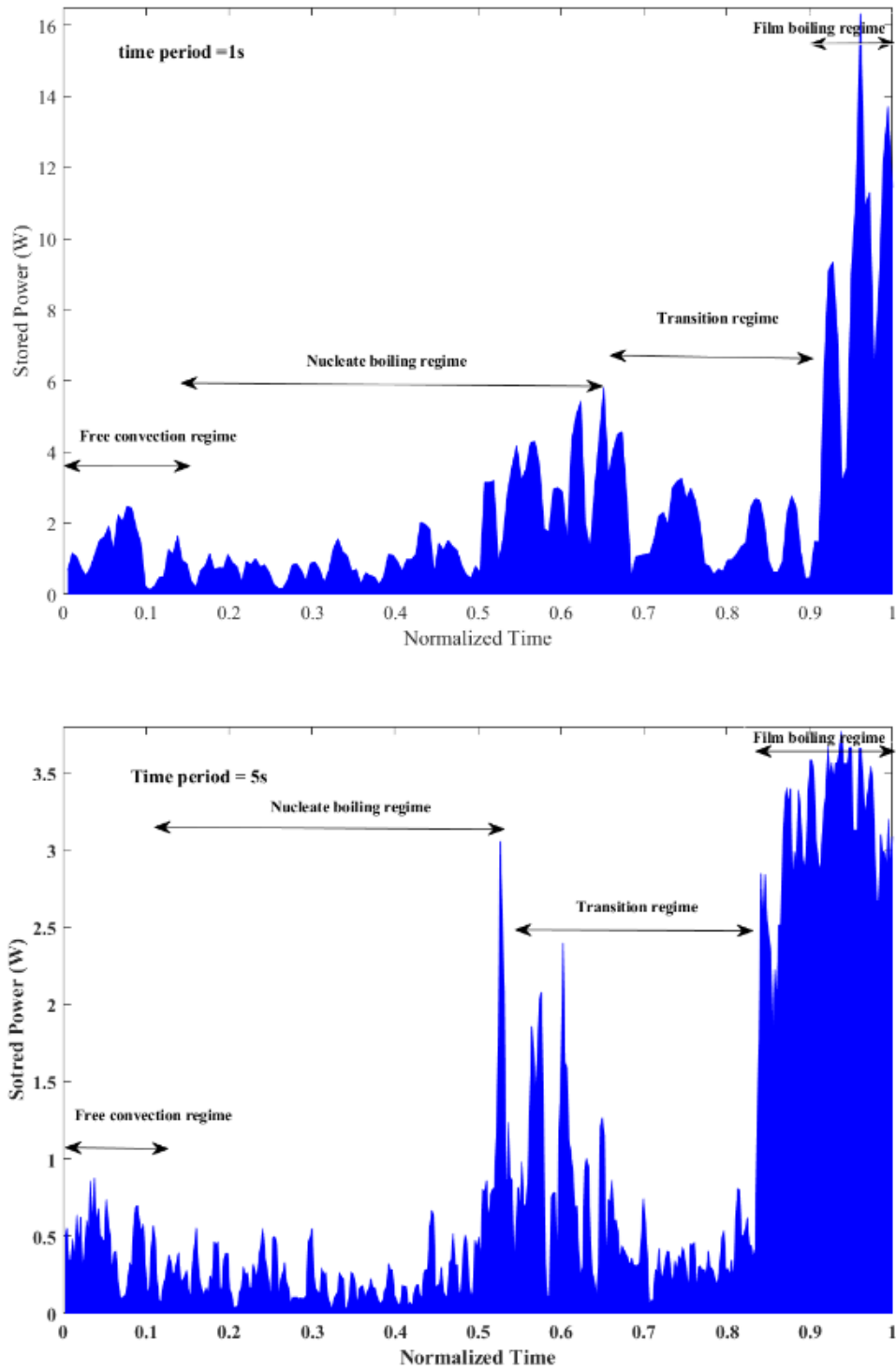
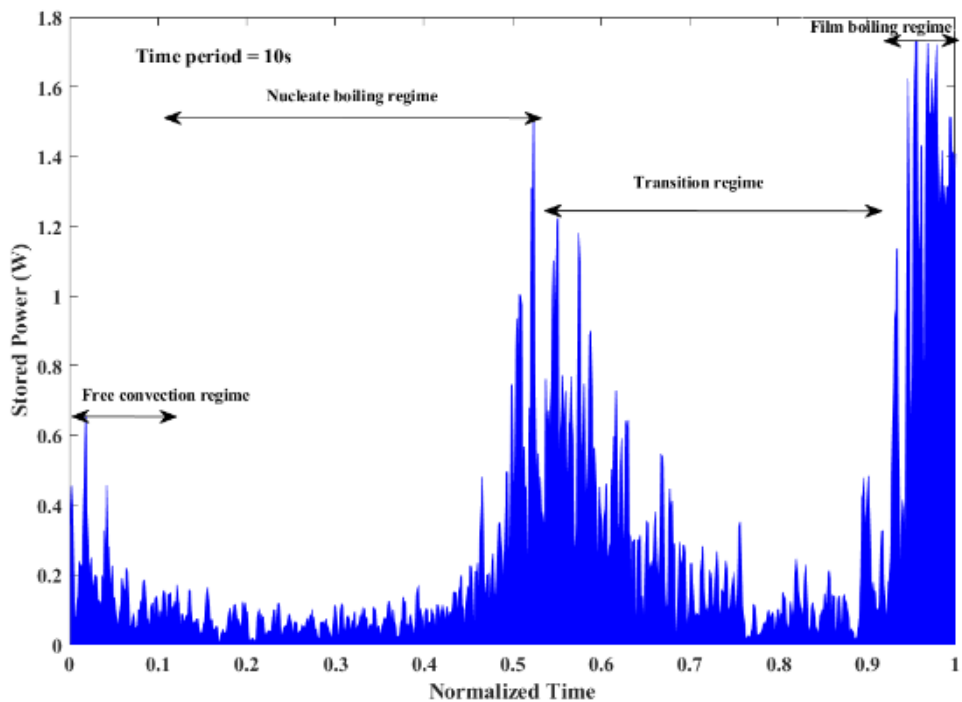**Fig. 5. stored energy rate at 1, 5, and 10s (Continued).**

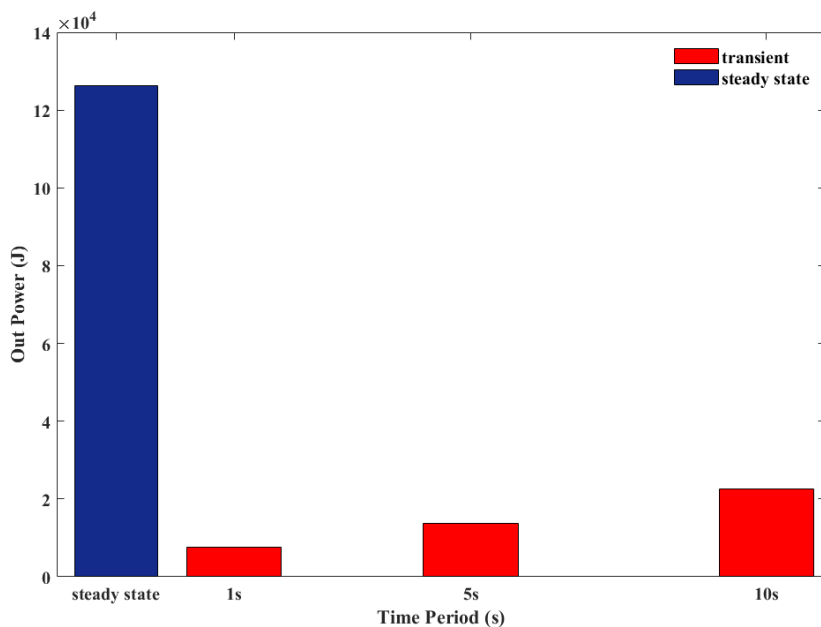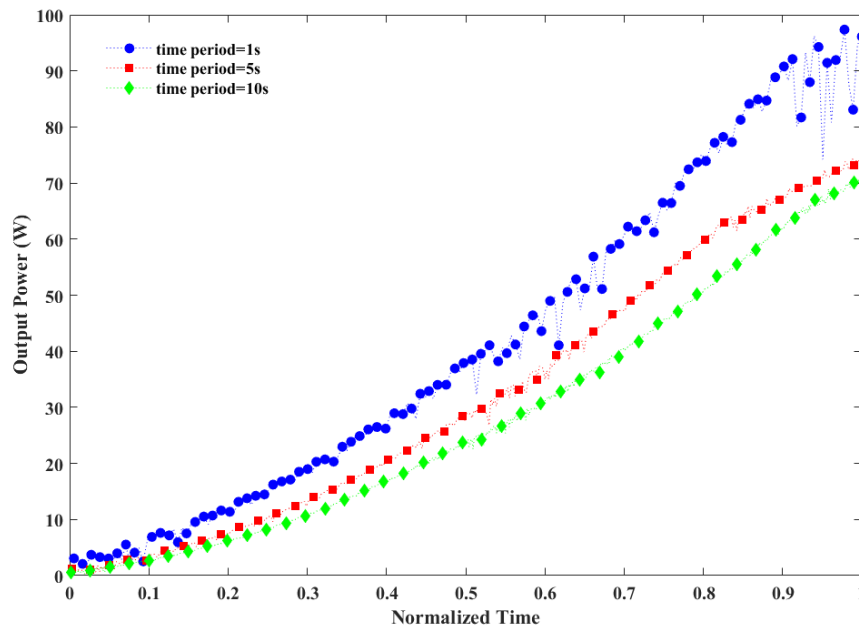**Fig. 5. stored energy rate at 1, 5, and 10s.**

Fig. 6. Output energy at the duration of 1, 5, 10s, and steady mode

Fig. 7. Output energy rate at duration of 1, 5, and 10s

Therefore, a higher decreasing heating rate, a higher increasing heat transfer. amount of output energy at duration of 5s is 81% higher than duration of 1s, and at duration of 10s is 65% higher than duration of 5s.

Output energy rate at duration of 1, 5, and 10s versus normalized time is shown in Fig. 7. Heating rate decreases with increasing duration. Output energy rate at the duration of 1s fluctuates higher than other durations due to high turbulence of bubble movements and higher density of growth and separation of bubbles than other durations. Fluctuations in output energy rate are high in transition regime and thicker part of vapor film in film boiling.

Vaporized water during experiments calculated from eq. (11) is shown in Fig. 8. Amount of vaporized water increases with increasing duration since output energy is increased. Although the output energy rate in duration of 1s is highest, the vaporized water amount is the lowest since output energy was low (Comparing Figs. 9 and 1·). Therefore, the vaporized water amount is high, which relates to experiment duration and consequently to output energy amount from wire than to heating rate.

Figs. 9 and 10 show the vaporized water rate for three durations. Vaporized water rate increases with decreasing duration, which matches the results of Fig. 8. At the beginning of the experiment, vaporized water is very low, showing a free convection regime since nucleate sites do not activate and no bubbles have been grown. As can be seen, vaporized water only follows output energy, which shows CHF mechanism is not affected by vaporized water. In addition, the slope of those

curves decreases in the experiment's last moment, indicating film thickness growth around the wire heater.

Fig. 11 shows the defined coolant performance in eq. (16) to observe coolant effectiveness for transient and steady modes of pool boiling. This figure shows that with increasing duration, coolant performance is enhanced, which shows deionized water in long duration is high and has a better ability to cool and receive energy from a wire heater. Its cause is related to nucleate sites' activity level, bubble growth duration, and bubble separation frequency. In long duration, they occur routinely without bubble coalescence and compression over the wire surface. In short duration, due to semi-explosive activity of nucleate sites and high bubbles with large scale, water's way to reach the wire surface becomes difficult, and as a result, transition and film boiling happen soon. In the steady mode of boiling, coolant performance is higher than in the transient mode (all durations), which indicates the excellent ability of working fluid to receive energy from wire. Also, behaviors between wire surface and deionized water, number of nucleate sites, and bubble growth rate in steady mode are more efficient than in transient mode.

Fig. 12 shows coolant performance versus normalized time for transient durations. As can be seen, first, coolant performance is low, which relates to the free convection regime, and heat transfer coefficient and bubbles had not formed yet. Next, coolant performance is enhanced, which coincides with the nucleate boiling regime. At the end of the nucleate boiling regime, CHF happens where heat transfer and performance are reduced. Reduction in performance
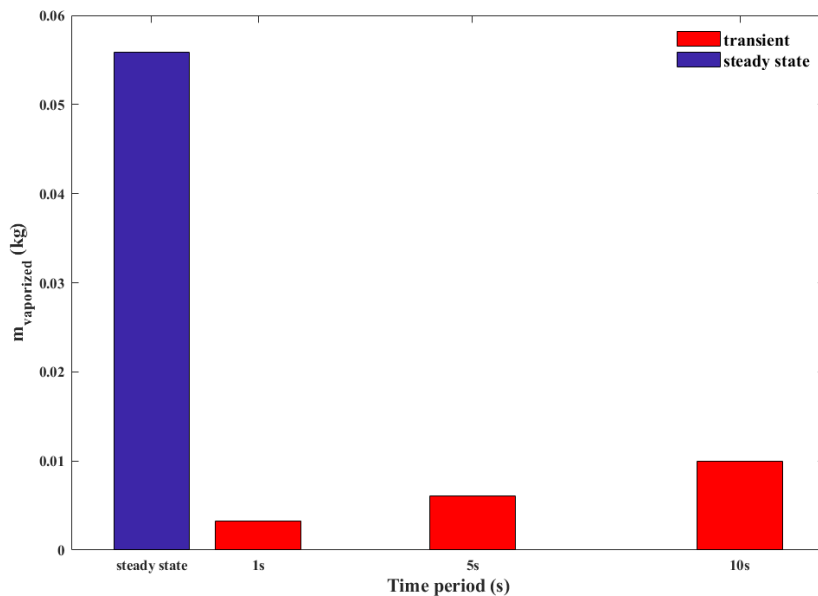
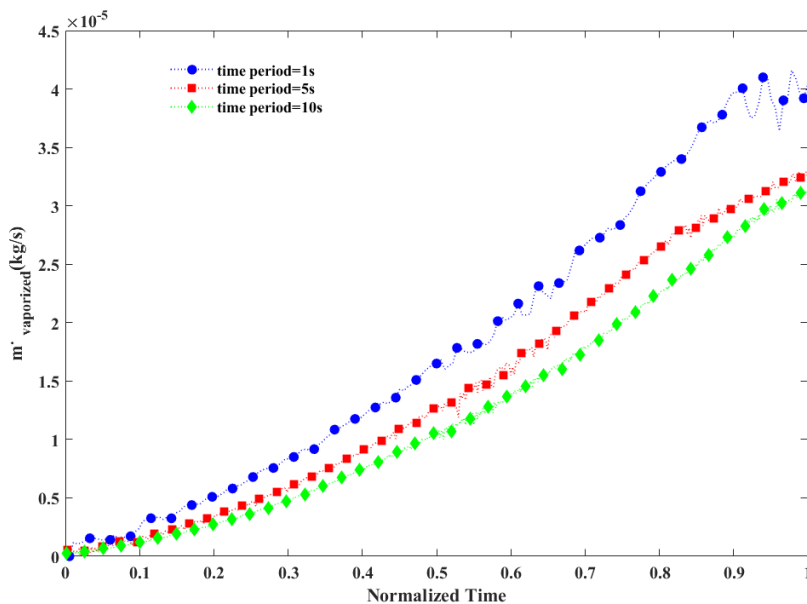**Fig. 8. vaporized water amount during experiments in transient and steady modes.**

Fig. 9. vaporized water rate versus normalized time for 1, 5, and 10s duration.
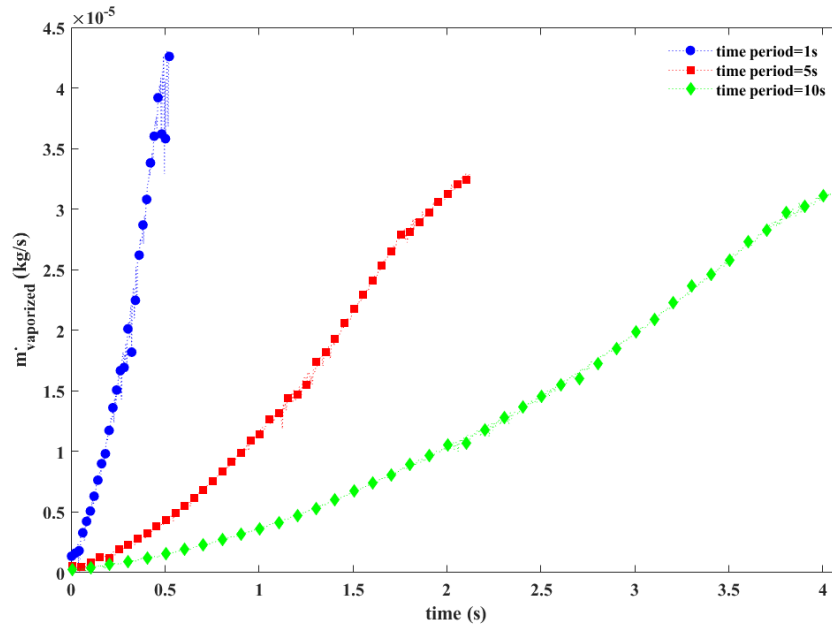
221

Fig. 10. vaporized water rate versus experiment duration for duration of 1, 5, and 10s
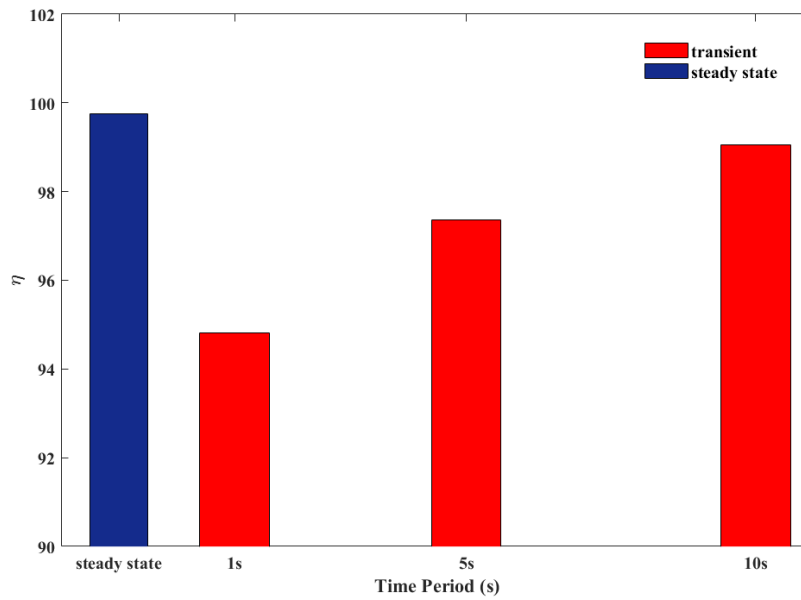

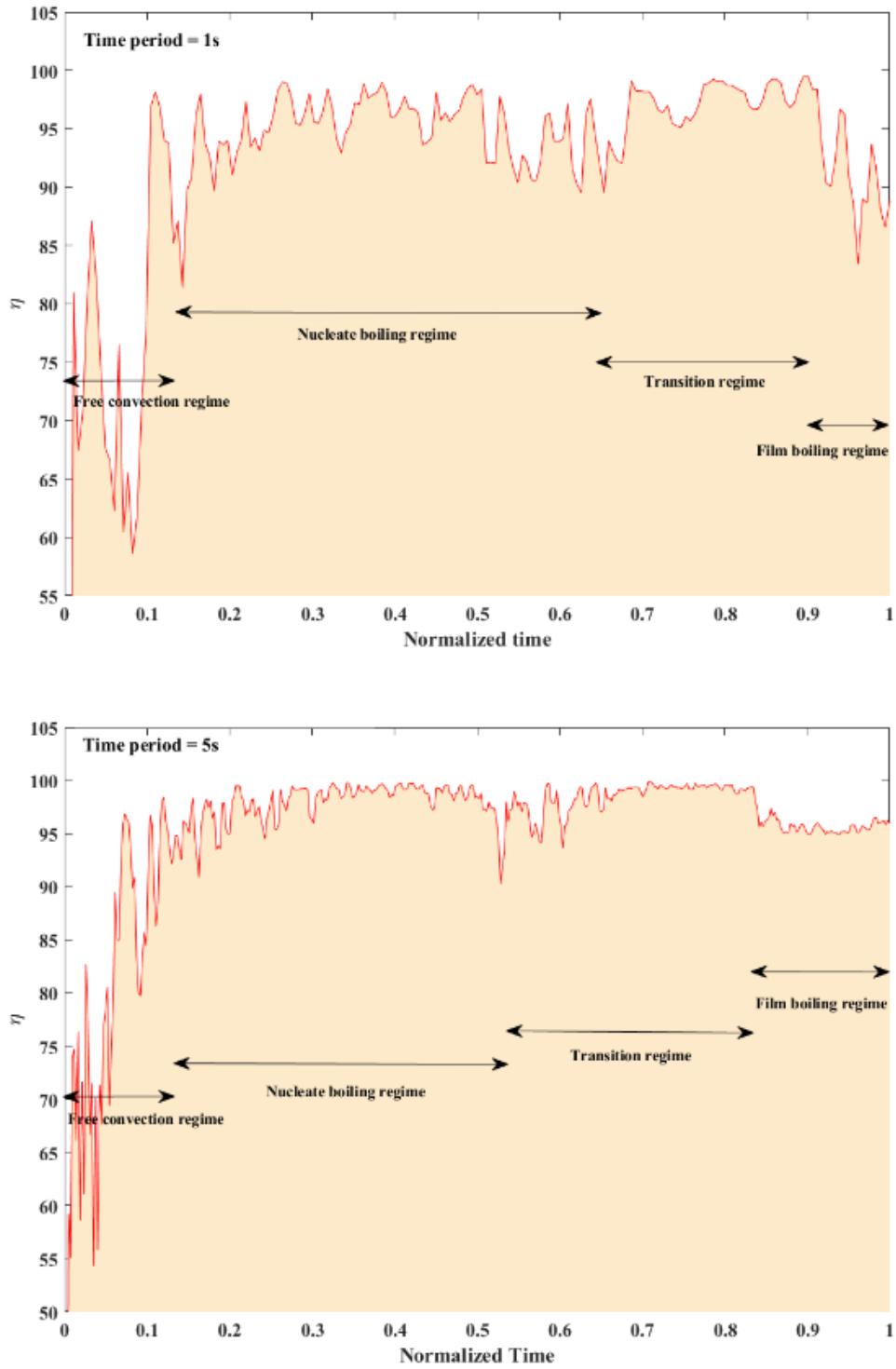**Fig. 11. Coolant performance of deionized water for the duration of 1, 5, 10s, and steady mode**

Fig. 12. Coolant performance versus normalized time for duration of 1s, 5s, and 10s(Continued).
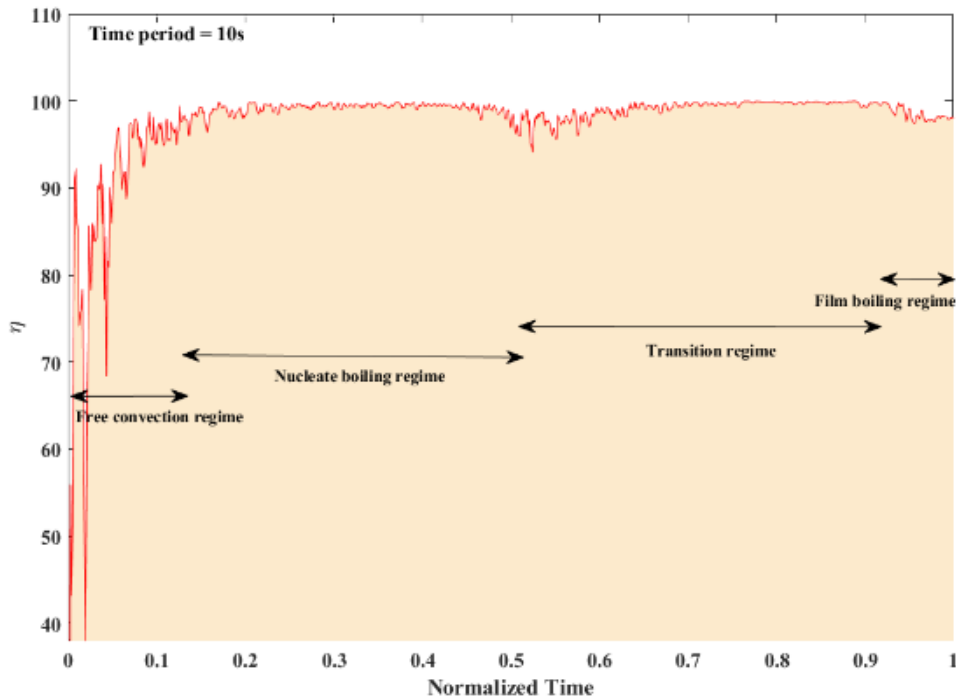
Fig. 12. Coolant performance versus normalized time for duration of 1s, 5s, and 10s.

continues in a transition regime where vapor film forms temporarily. Then, performance increases and becomes nearly constant with time at the beginning of film boiling. Finally, even though radiation heat transfer is higher than other moments, performance reduces in the thick part of vapor film in film boiling.

4- Conclusion

In systems that deal with the amount of heat, its analysis is often examined in terms of the amount of heat transfer, while another method is to investigate energy analysis. Different definitions of coolant performance and their effectiveness can be provided. In this research, some relations have been extracted for an in-depth study of the effectiveness of pool boiling. In the transient mode of pool boiling, the stored energy value is decreased with increasing duration. As a result, in 5s duration, stored energy is reduced by 10% compared to the duration of 1s, while in the duration of 10s, stored energy is reduced by 42% compared to the duration of 5s. The amount of energy stored in steady mode for durations of 1s and 5s is lower than in transient mode, which indicates an increase in heat transfer in steady state compared to transient state for short durations. The amount of energy stored in steady mode for 1s and 5s durations is lower than in transient mode, which indicates short durations. In a short duration, heat transfer in steady mode increases compared to transient mode. Duration can be scheduled and optimized to store less energy, and as a result, high output is less from the wire heater in the transient mode of boiling. As duration decreases, inactive or semi-active nucleate sites suddenly become fully active. Output energy rate at the duration of 1s fluctuates more than other durations due to the high turbulence of bubbles' movements, higher growth, semi-explosive nucleate generation, and separation of bubbles. Fluctuations in output energy rate are high in the transition regime and thicker part of vapor film in film boiling (second part of film boiling). In short duration, due to semi-explosive activity of nucleate sites and high bubbles with large scale, water's way to reach wire surface becomes difficult. As a result, transition and film boiling happens soon. Although radiation heat transfer is more activated in film boiling than in other regimes, performance reduces in the thick part of vapor film. Finally, it is a good subject that in future research, the amount of increase in thickness of vapor film around the wire and its changes at different durations and in the steady state be investigated.

References

[1] a. ayoobi, A. Faghih Khorasani, M.R. Tavakoli, effects of subcooled temperatures on transient pool boiling of deionized water under atmospheric pressure, AUT Journal of Mechanical Engineering, 4(1) (2020) 67-78.

[2] A. Ayoobi, A.F. Khorasani, M. Barzegar, M.H.N. Zavare, Experimental study on effects of water hardness during transient pool boiling and development of an artificial neural network, International Journal of Heat and Mass Transfer, 227 (2024) 125563.

[3] A. Ayoobi, A. Faghih Khorasani, Study of transient pool

boiling of deionized water in two modes of presence and absence of a magnetic field, Journal of solid and fluid mechanics, 10(1) (2020) 209-221.

[4] A. Ayoobi, A.F. Khorasani, M. Ramezanizadeh, A. Afshari, Experimental investigation of transient pool boiling characteristics of Fe3O4 ferrofluid in comparison with deionized water, Applied Thermal Engineering, 179 (2020) 115642.

[5] A. Ayoobi, A.F. Khorasani, M.R. Tavakoli, M.R. Salimpour, Experimental study of time period of continued heating rate on pool boiling characteristics of saturated water, International Journal of Heat and Mass Transfer, 137 (2019) 318-327.

[6] S. Deb, S. Pal, D.C. Das, M. Das, A.K. Das, R. Das, Surface wettability change on TF nanocoated surfaces during pool boiling heat transfer of refrigerant R-141b, Heat and Mass Transfer, 56(12) (2020) 3273-3287.

[7] P. Naphon, C. Thongjing, Pool boiling heat transfer characteristics of refrigerant-nanoparticle mixtures, International Communications in Heat and Mass Transfer, 52 (2014) 84-89.

[8] B.D. Bock, M. Bucci, C.N. Markides, J.R. Thome, J.P. Meyer, Pool boiling of refrigerants over nanostructured and roughened tubes, International Journal of Heat and Mass Transfer, 162 (2020) 120387.

[9] M. Kim, S.J. Kim, A mechanistic model for nucleate pool boiling including effect of bubble coalescence on area fractions, International Journal of Heat and Mass Transfer, 163 (2020) 120453.

[10] R.K. Gouda, M. Pathak, M.K. Khan, Pool boiling heat transfer characteristics of a biosurfactant particle deposited heating surface, International Journal of Heat and Mass Transfer, 163 (2020) 120455.

[11] S.M.S. Murshed, K. Vereen, D. Strayer, R. Kumar, An experimental investigation of bubble nucleation of a refrigerant in pressurized boiling flows, Energy, 35(12) (2010) 5143-5150.

[12] S. Shin, G. Choi, B.S. Kim, H.H. Cho, Flow boiling heat transfer on nanowire-coated surfaces with highly wetting liquid, Energy, 76 (2014) 428-435.

[13] Z. Li, A. Mazinani, T. Hayat, A.A.A.A. Al-Rashed, H. Alsulami, M. Goodarzi, M.M. Sarafraz, Transient pool boiling and particulate deposition of copper oxide nano-suspensions, International Journal of Heat and Mass Transfer, 155 (2020) 119743.

[14] G. Righetti, L. Doretti, H. Sadafi, K. Hooman, S. Mancin, Water pool boiling across low pore density aluminum foams, Heat Transfer Engineering, 41(19-20) (2020) 1673-1682.

[15] A.R. Betz, J. Jenkins, C.-J.C. Kim, D. Attinger, Boiling heat transfer on superhydrophilic, superhydrophobic, and superbiphilic surfaces, International Journal of Heat and Mass Transfer, 57(2) (2013) 733-741.

[16] J. Li, G. Zhu, D. Kang, W. Fu, Y. Zhao, N. Miljkovic, Endoscopic Visualization of Contact Line Dynamics during Pool Boiling on Capillary-Activated Copper Microchannels, Advanced Functional Materials, n/a(n/a) (2020) 2006249.

[17] M.R. Mata Arenales, S.K. C.S, L.-S. Kuo, P.-H. Chen, Surface roughness variation effects on copper tubes in pool boiling of water, International Journal of Heat and Mass Transfer, 151 (2020) 119399.

[18] P. Zakšek, M. Zupančič, P. Gregorčič, I. Golobič, Investigation of Nucleate Pool Boiling of Saturated Pure Liquids and Ethanol-Water Mixtures on Smooth and Laser-Textured Surfaces, Nanoscale and Microscale Thermophysical Engineering, 24(1) (2020) 29-42.

[19] R.J. Moffat, Describing uncertainties in experimental results, Experimental thermal and fluid science, 1(1) (1988) 3-17.

[20] W.M. Rohsenow, A method of correlating heat transfer data for surface boiling of liquids, Cambridge, Mass.: MIT Division of Industrial Cooporation,[1951], 1951.

[21] N. Zuber, Nucleate boiling. region of isolated bubbles and similarity with natural convection, International Journal of Heat and Mass Transfer, 6(1) (1963) 53-78.

[22] I. Sedmak, I. Urbančič, J. Štrancar, M. Mortier, I. Golobič, Submicron thermal imaging of a nucleate boiling process using fluorescence microscopy, Energy, 109 (2016) 436-445.